Chapter 4

Outage-Constrained Energy Harvesting Based Relay Selection

With the requirement of ultra-low latency and ultra-high reliability, the energy efficient design is also a necessity of time for the 5G communication systems [60]. Furthermore, the deployment of ultra-dense communication nodes to meet the demand of cellular traffic in the 5G communication system poses a high CO_2 emissions threat [61]. Therefore to contribute to one of the SDG, the recent interest in energy efficient system designs has enhanced manifold. Hence in this chapter, we consider a RF-EH relay-assisted cooperative D2D communication system. For such a system, we propose an energy efficient outage-constrained energy harvesting based relay selection (OC-EHRS) policy.

The green cooperative D2D communication system model along with the proposed relay selection policy is discussed briefly in Section 4.1. In Section 4.2, we present statistical analysis for average maximum harvested energy by EH relay nodes. Further, in Section 4.3, we describe the outage contained transmission of the best selected relay in the system model considered. For the performance analysis of the proposed policy, we evaluate outage probability, FASE, and FAEE in Section 4.4, 4.5, and 4.6, respectively. Section 4.7 presents the numerical results and comparison of the proposed policy with the benchmark policies. Lastly in Section 4.8, we present the summary of the chapter. The proof of all the results is relegated in Appendix C.

4.1 Green Cooperative D2D System Model

A green cooperative D2D wireless system shown in Figure 4.1 is considered in this chapter. In it, source node S needs to send the information to the destination node D via two-hop statistically independent wireless fading channels. We assume the absence of a direct link between the transmitting source node S and the destination node D [97]. For each timeslot T, the relay that harvests the maximum energy among the L relay nodes is selected to forward its received signal to node D. In the multi-EH system, we consider L RF-EH non-regenerative relay nodes [115], which are denoted

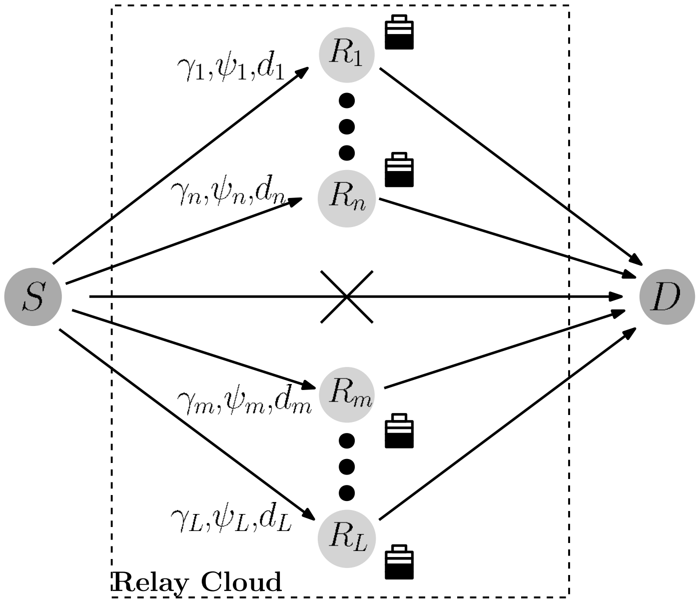

Figure 4.1: EH multi-relay assisted, green cooperative D2D system model.

as $R_1, R_2, \ldots, R_L$, and $d_1, d_2, \ldots, d_L$ denotes the distances between the source node and EH relay nodes (EHRNs), respectively. We also assume that each EHRN has a sufficient energy storage facility, and all the nodes in the system model have a single antenna for half-duplex transmission and reception [96].

Note that only the selected RF EHRN assists the source node in forwarding its data. However, the selected relay transmits or does not transmit based on the channel conditions. Therefore, the communication policy that we propose considers the CSI of both the hops. Furthermore, each EH node harvests RF energy from the incoming source signal and consumes this harvested RF energy to forward its received signal to the destination node [116]. We also assume that the source node and the destination node has sufficient energy resources; that is, there is no power constraint [115].

Source and the first hop channels: Let P_s is the average source transmit power. We assume that the source node is a non-EH node [67]. Further, we assume quasi-static frequency-flat Rayleigh fading channels between source node to EHRNs [96]. Let $\gamma_1, \gamma_2, .., \gamma_L$ represent the instantaneous channel power gains of $S - R_n (n = 1, 2, \ldots, L)$ links, respectively. We assume that the channels are statistically independent [116, 117]. However, the channels need not be identical.

In the proposed green cooperative D2D EH model, we consider time-switching protocol (TSP). Note that implementing TSP leads to a system with perfect synchronization and reduced complexity [116, 118]. We assume that the processing power required for EHRNs is very small and negligible [116, 119]. We present details on TSP based transmission policy, EH based relay selection, and the second hop outage-constrained transmission in the following sections.

Remarks on model and its extensions and practical application: In the EHRNs assisted cooperative wireless system model, we consider only one source-destination pair. However, different system model extensions are indeed possible. For instance, the green cooperative system having multiple source-destination pairs, a green cooperative system having nodes equipped with multiple antennas. For such complex models, the communication protocols would be more complicated because of issues such as synchronization, resource allocation and channel estimation.

Furthermore, it is also possible to have a model where the source and destination nodes have EH capabilities. However, such fully EH models have intermittent applications due to the EH nature of the nodes. There are possible use cases where only the relays are EH-based, but the source and destination nodes are not. For example, in the EH or hybrid unmanned aerial vehicle (UAV)-assisted cooperative communication system [120], where source and destination are at the ground location with sufficient power supply; however, UAV which is acting as a relay will require harvested energy from radio frequency (RF) signals to forward its received signal to the destination. In such cases, it is essential to have relays with RF energy harvesting capabilities. However, the non-EH source and the destination already have sufficient energy resources and can radiate strong RF signals towards the EH UAVs. Techniques such as SWIPT are useful in designing green cooperative networks. Furthermore, hybrid EH relays that use the solar or wind-based EH mechanisms are useful for some applications; however, adding complexity.

4.1.1 Time-Switching Based Transmission Protocol

TSP comprises of two essential tasks, namely, EH and information transmission. All the EHRNs in the system follow TSP. Figure 4.2 shows a timeslot of TSP based communication policy. In it, T denote the timeslot duration, which comprises of three sub-timeslots, which are of duration $\frac{(1-\upsilon)}{2}T$, υT, and $\frac{(1-\upsilon)}{2}T$, respectively. The first sub-timeslot $\frac{(1-\upsilon)}{2}T$, is the sub-timeslot for data transmission from source to EHRNs. The second sub-timeslot υT is the fraction of time for which EHRN harvest energy from the received RF signal. Lastly, the third sub-timeslot $\frac{(1-\upsilon)}{2}T$ is another data transmission sub-timeslot for the selected EH relay to forward information.

Remarks on sub-timeslot υT: Note that the fraction υ serves as information transmission versus EH tradeoff parameter. The system engineer has to choose υ carefully. For instance, selecting the υ value such that an outage probability of about 1% is achievable [100]. It is possible to optimize the green cooperative D2D system with optimum υ. However, we focus on designing energy efficient communication policy and its performance analysis for cooperative D2D wireless systems wherein the nodes would have only partial CSI [121].

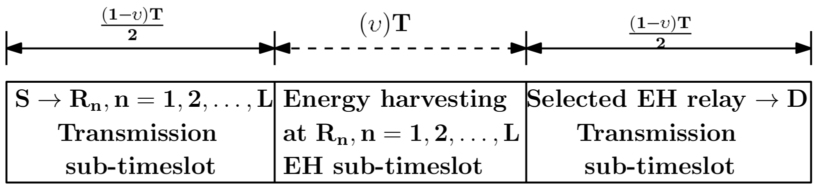

Figure 4.2: Illustrating a timeslot in the time-switching based energy efficient relaying policy.

Remarks on time synchronization problem: Note that it is true that TSP has synchronization problems. However, we would like to emphases on the fact that integrating robust synchronization algorithms [122] can help in efficiently estimating the offset and provide the compensating circuitry for the correction of offsets and hence sampling at optimal times.

Remarks on trade-off between the TSP and power splitting protocol (PSP): For the proposed system model with EH capable relays, we have considered a TSP for SWIPT. However, a PSP also exists for SWIPT. Following is the trade-off between the TSP and PSP for the proposed model.

- In TSP, the relay antenna is connected with EH circuitry, often called a rectenna, and signal decoding circuitry. Further, time synchronization mechanisms are used to control signals applied to these circuits [123]. Since successive circuits are used for EH and signal decoding, the signal transmission will take more time when compared to PSP. However, TSP allows for simple hardware implementation [124].

- In PSP, the antenna is connected to both EH circuitry and signal decoding circuitry. Thus signal received by the antenna is shared between both EH and signal decoding circuits [123]. Note that energy harvesting and signal decoding are done concurrently. Therefore, the transmission time taken by PSP is less than TSP. However, PSP entails more complex hardware implementation [124].

Note that the hardware implementation complexity of TSP is low. Further, the commercial availability of the TSP circuitry is more in comparison to PSP [123]. Therefore, we have considered TSP in our system model.

4.1.2 EH Relay Node Tasks: Harvesting and Transmission

EHRN consists of two subsystems, namely, EH subsystem (EHSS) and information processing subsystem (IPSS). The main task of EHSS is to rectify the received RF signal and to store the energy. The RF-EH circuits are assumed to be highly sensitive. IPSS, on the other hand, manages down-conversion of RF-to-baseband signal and baseband signal processing. Note that all the harvested energy by EHRNs in υT duration is used to forward the data signal to the destination [116].

Remarks on EHRN and EH process: In this chapter, we consider non-regenerative EH relay nodes, given its simplicity and ease of implementation. Therefore, these relays require minimal processing by the IPSS. Further, we assume that the EH relay uses its harvested energy in the sub-timeslot for information transmission within that timeslot T. Note that due to the time-varying fading channel, the energy harvested by an EHRN is random.

4.1.3 EH based Relay Selection and Remarks

We propose an energy efficient or green cooperative D2D communication policy that consists of a simple EH relay selection policy, and outage-constrained energy conserving relaying policy. While the former reduces the CSI requirement significantly, the latter conserves energy by allowing the selected EHRN to transmit based on channel conditions. We state the EH relay selection policy as follows. Let $\mathcal{EH}_1, \mathcal{EH}_2, \ldots, \mathcal{EH}_L$ denote the harvested energies by the L EHRNs during the time υT. We choose the relay that harvests maximum energy, that is, choose the EHRN $R_{\mathbb{S}}$ when

$$\mathbb{S} = \arg \max_{1,2,\ldots,L} \mathcal{EH}_m. \tag{4.1.1}$$

Remarks on EH relay selection: We note that for each timeslot T, the non-selected EH relay may have some amount of residual energy. We assume that the non-selected EHRN uses its residual energy for low-data transmission to some other destination. Therefore, at the end of each timeslot, all energy storing subsystems of EHRNs will be empty [125].

We use the order statistics approach for ordering the continuous random variables. For the Rayleigh fading model, the harvested energies, which depend on instantaneous channel power gains, are exponentially distributed. Let $\mathcal{EH}_n$ denote the maximum energy harvested by the n^{th} EH relay node. Suppose that k^{th} $(n \neq k)$ EH relay node also harvest the same amount of energy, denoted by $\mathcal{EH}_k$. Note that $\mathcal{EH}_n$ and $\mathcal{EH}_k$ represent two continuous random variables. Now, consider the probability of these two relays harvesting equal energy, that is $\mathcal{P}(\mathcal{EH}_n = \mathcal{EH}_k)$ is zero. Because, $\mathcal{P}(\mathcal{EH}_n = \mathcal{EH}_k) = \int\int_{\mathbb{A}} p_{\mathcal{EH}_n}(u)\ p_{\mathcal{EH}_k}(v)\ \mathrm{d}u\ \mathrm{d}v$, where $\mathbb{A} = \{(u, v) \in \mathbb{R}^2 : u = v\}$, has area zero [38]. Thus, we conclude that, in probabilistic sense, it is not possible to have two relays harvesting maximum amount of energy. However, it is indeed possible to select a subset of L EH relays as described below.

Extensions–Subset of L EH relays selection: Unlike selecting a single EH relay that harvests maximum energy, it is possible to choose a subset M of L relays ($M < L$) based on the certain harvested energy threshold. However, the subset of L EH relays selection would cause synchronization problems in synchronous or coherent green cooperative D2D communication systems. In addition to timing and frequency synchronization challenges, the selection of more EH relays would increase hardware complexity and the burden of acquiring more CSI. Increased CSI requirement would lead to higher pilot overhead and hence more energy consumption. Therefore, subset relays selection is neither spectrally efficient (due to large pilot overhead) nor energy efficient (due to enhanced transmissions) in green cooperative D2D radio systems. Moreover, the subset EH relays selection based on the threshold is beyond our proposed work scope. The subset EH relays selection, and outage-constrained relaying policy and its performance analysis could be potential future work.

We note that the above relay selection policy uses only instantaneous and partial CSI of the channels between the source and the EHRNs. The proposed relay selection policy is useful in practical cooperative D2D wireless systems wherein the nodes would have only one hop or partial CSI [121]. We assume that the selected non-regenerative EHRN is always active and has sufficient harvested energy to forward the signal to the destination. Furthermore, to choose the EHRN that harvest maximum energy, in addition to CSI, the knowledge of other parameters such as distances, path loss exponent, harvesting duration, are also essential for computing the harvested energies. We assume that this knowledge is available to the source node.

However, the novelty of the communication policy lies in the energy conserving nature of the relaying policy. In it, the selected relay $R_{\mathbb{S}}$ forwards its received signal only when the channel power gain between $R_{\mathbb{S}}$ and destination node is above a specific threshold. Based on fading channel outage, we determine the threshold as a function of outage probability. We now present remarks on the CSI requirements of various nodes below.

4.1.4 Remarks on CSI

The CSI requirements of the proposed green cooperative D2D communication system are as follows.

- *Source CSI requirement:* The source S requires instantaneous CSI of the links between the source node to all the EHRNs. This CSI is useful for determining the strongest EHRN, which forwards the signal to the destination node based on the channel conditions. Therefore, for relay selection, the node S requires partial instantaneous CSI. One approach for CSI acquisition is as follows. The EHRN estimates the CSI between itself and the source node based on known pilot signals and sends the estimated CSI back to the source node by exploiting channel reciprocity. However, this conventional method of channel estimation requires a dedicated battery that does not rely on RF-EH [126].

Alternatively, a more practical solution of CSI acquisition in the energy constrained network is presented in [127]. In [127], the source node acquires CSI from a one-bit feedback algorithm. In this algorithm, on receiving the information symbol at the relay for EH, it sends a one-bit feedback signal based on the energy level higher than or lower than the previously received information symbol. Further, based on received feedback bit, the channel is estimated using a specific optimization technique.

- *EHRN CSI requirement:* The EHRNs do not require CSI between themselves and the source. This non-requirement of CSI is because the EHRN acts as a non-regenerative repeater and does not do any additional processing. Therefore, EHRN implementation is relatively simple and practically amenable. However, the selected EH relay requires CSI between itself and the destination link and channel outage parameter to determine the channel state for further transmission.

- *Destination node CSI requirement:* We assume that at the end of the timeslot T, the destination receiver performs ML detection. For decoding, the destination node D requires instantaneous CSI of two fading channels, namely, the CSI between the source to the selected EHRN, and between the selected EH relay node and the destination node. Note that the CSI acquisition process remains the same as adopted by the source node.

Remarks on the overhead and CSI complexity of the selected EH relay: Note that, there is some computational overhead on the selected EH relay. The EH relay has to compute the outage probability, a function of the threshold and average CSI. Based on the outage probability computed, the selected EH relay will decide whether to transmit or not. We discuss the following possible scenarios for the CSI acquisition.

- *Scenario 1–Pilot transmission by the destination node:* The overhead issue arises when the EH relay uses pilots (known energy sequences, PN sequences, for example) for the acquisition of CSI. However, in the scenario where the destination node sends the pilots to the relay [128], there will not be any overhead burden on the selected EH relay in the form of pilots transmission.

- *Scenario 2–Pilot transmission by battery-equipped EH relay:* Alternatively, the EH relays, to acquire CSI, can be equipped with a limited battery for pilot transmission [129]. The battery energy is used for CSI acquisition and will not be available for signal transmission. The OC-EHRS policy is less complex because it requires average CSI than instantaneous CSI.

Further, in the upcoming sections, we provide the performance analysis of the proposed policy in green cooperative D2D communication network which is non-trivial, and novel. Furthermore, the analytical results that we derive serve as a valuable benchmark for EH cooperative D2D relay systems.

4.2 Order Statistics of Green Cooperative D2D Model

In this section, we develop an insightful statistical analysis for average maximum harvested energy by EHRNs. The EHRNs harvest energy from the source RF signal transmissions. Therefore, harvested energy is the function of source transmit power and TSP parameters. We assume that υ and T are the same for all the EHRNs. The path loss effect due to separation between the source and EHRNs is deterministic, and the range for path loss exponent is $2 \leq \nu \leq 7$, which cover different wireless propagation environments [100]. Furthermore, η is the energy conversion efficiency, which is the same for all EHRNs.

Remarks: Note that due to the non-linear circuit elements used for RF-DC conversion, the linear relationship will not exist between input RF and output harvested power. However, the research work conducted in this thesis is not focused on the circuit perspective. Instead, it focuses on studying the random nature of the energy harvested by the relays in the cooperative EH network. Accounting for the non-linearity of the energy harvesting profile makes the model more complex and analytically intractable and can be a potential future work.

4.2.1 Large Scale Plus Small Scale Fading Model

The fading model, which is under consideration, accounts for multi-path fading effects, shadow fading, and path loss. Let $Y_n \sim \mathcal{N}(0, \sigma_n^2)$. When the generalised fading model is used, the instantaneous energy harvested at a specific EHRN (R_n) is given by

$$\mathcal{EH}_n = \frac{\eta P_s \gamma_n}{d_n^{\nu} \psi_n} \upsilon T, \tag{4.2.1}$$

where $\psi_n = 10^{\frac{Y_n}{10}}$, which denotes a log-normal random variable, and γ_n, which denotes an exponential random variable, are statistically independent. Let $\mathbf{E}[\gamma_n] = \overline{\gamma}_n$. The average energy harvested at n^{th} relay node R_n is given by

$$\overline{\mathcal{EH}_n} = \frac{\eta P_s \overline{\gamma}_n \upsilon T}{d_n^{\nu}} \mathbf{E}\left[\frac{1}{\psi_n}\right]. \tag{4.2.2}$$

We state the following result on the statistical average of $\mathbf{E}[\max\{\mathcal{EH}_1, \ldots, \mathcal{EH}_L\}]$ for the general fading scenario.

Lemma 4.2.1 *Let* $\zeta_n \triangleq \frac{\eta P_s}{d_n^{\nu}} \upsilon T$*, which implies,* $\overline{\mathcal{EH}_n} = \zeta_n \overline{\gamma}_n \mathbf{E}\left[\frac{1}{\psi_n}\right]$*. Further, let the maximum energy harvested by the EH relay node can be written as*

$$\mathcal{EH}_{\max} = \max\{\mathcal{EH}_1, \mathcal{EH}_2, \ldots, \mathcal{EH}_L\} \tag{4.2.3}$$

Therefore, the statistical average of the continuous random variable $\mathcal{EH}_{\max}$ *is expressed as*

$$\overline{\mathcal{EH}}_{\max} = \int_0^{\infty} \left(1 - \prod_{n=1}^{L} Q\left(\frac{\epsilon}{\sigma_n} \ln\left(\frac{\zeta_n}{y}\right)\right)\left(1 - e^{-\frac{y}{\overline{\gamma}_n}}\right)\right) dy. \tag{4.2.4}$$

Suppose the separation between the source node and all the EHRNs be equal, that is $d_1 \approx d_2 \approx \ldots \approx d_L = d$, $\mathbf{E}\left[\frac{1}{\psi_1}\right] = \mathbf{E}\left[\frac{1}{\psi_2}\right] = \ldots = \mathbf{E}\left[\frac{1}{\psi_n}\right] = \ldots = \mathbf{E}\left[\frac{1}{\psi_L}\right] = \mathbf{E}\left[\frac{1}{\psi}\right]$ *and* $\sigma_1 = \ldots = \sigma_n = \ldots = \sigma_L = \sigma$*. Furthermore, assuming all the mean channel power gain of the source node to EHRNs links are equal, that is* $\overline{\gamma}_1 = \overline{\gamma}_2 = \ldots = \overline{\gamma}_n = \ldots = \overline{\gamma}_L = \overline{\gamma}$*, and* $\zeta_1 \approx \ldots \approx \zeta_n \approx \ldots \approx \zeta_L = \zeta$*. Therefore, we have*

$$\overline{\mathcal{EH}}_{\max} = \int_0^{\infty} \left(1 - \left(Q\left(\frac{\epsilon}{\sigma} \ln \frac{\zeta}{y}\right)\right)^L \left(1 - e^{-\frac{y}{\overline{\gamma}}}\right)^L\right) dy, \tag{4.2.5}$$

$$= \int_0^{\infty} \left(1 - \left(\frac{1}{2} erfc\left(\frac{\epsilon}{\sigma\sqrt{2}} \ln \frac{\zeta}{y}\right)\right)^L \left(1 - e^{-\frac{y}{\overline{\gamma}}}\right)^L\right) dy, \tag{4.2.6}$$

where $\epsilon = \frac{10}{\ln 10}$*, erfc is the complementary error function. Further, for* $L = 1$*, we get* $\overline{\mathcal{EH}}_{\max} = \zeta e^{\frac{\sigma^2}{2\epsilon^2}} \overline{\gamma} \triangleq \overline{\mathcal{EH}_1}$*. The proof of the above expression is relegated in appendix C.1.*

Remarks: We can numerically evaluate the above single integral expression. In the absence of shadow fading, we ignore the ψ random variable, which implies Rayleigh fading with the simplified path loss model. On the other hand, in the absence of multipath fading, we have only a large scale fading model. The average maximum harvested energy $\overline{\mathcal{EH}}_{\max}$ increases with the increase in the number of EH relays. Assuming all other parameters fixed, as the mean channel power gain $\overline{\gamma}$ increases, $\overline{\mathcal{EH}}_{\max}$ increases, as expected. For $L = 1$, $\overline{\mathcal{EH}}_1$ serves as a lower bound. Thus, we have a trade-off between EH cooperative D2D system complexity and the mean harvested energy $\overline{\mathcal{EH}}_{\max}$. We numerically evaluate the $\overline{\mathcal{EH}}_{\max}$ in section 4.7.

4.3 Outage-Constrained Relay Transmission

The relay selection policy for the first hop selects the strongest EHRN, which requires partial instantaneous CSI. We now extend the communication policy by considering relay to destination link CSI. If the selected EH relay to destination node channel quality is very poor, the transmitted signal will experience deep fade with high probability. Therefore, in such deep fade scenarios, the selected EHRN should conserve the harvested energy by avoiding transmissions.

We propose the following energy conservation rule based on the link outage defined on instantaneous channel power gain. Mathematically, the selected EH relay sets

$$\mathcal{A} = \begin{cases} 1, & \gamma_{r_{\mathbb{S}}d} \geq \gamma_0, \\ 0, & \text{otherwise.} \end{cases} \tag{4.3.1}$$

where $\mathcal{A}$ acts as the indicator of the relay transmission, $\gamma_{r_{\mathbb{S}}d}$ is the channel power gain of $R_{\mathbb{S}} - D$ link and γ_0 is the threshold for the channel power gain of the $R_{\mathbb{S}} - D$ link. We call $\mathcal{A}$ as the energy conserving parameter of the policy.

The expression for γ_0 is obtained by deriving outage probability, that is, $p_0 \triangleq \mathcal{P}(\gamma_{r_{\mathbb{S}}d} < \gamma_0)$. Therefore, the outage probability is given by

$$p_0 = \frac{1}{\overline{\gamma}_{r_{\mathbb{S}}d}} \int_0^{\gamma_0} e^{-\frac{\gamma_{r_{\mathbb{S}}d}}{\overline{\gamma}_{r_{\mathbb{S}}d}}} \, \mathrm{d}\gamma_{r_{\mathbb{S}}d}, = 1 - e^{-\frac{\gamma_0}{\overline{\gamma}_{r_{\mathbb{S}}d}}}. \tag{4.3.2}$$

Further simplification yields the following expression for threshold.

$$\gamma_0 = \overline{\gamma}_{r_{\mathbb{S}}d} \ln\left(\frac{1}{1 - p_0}\right), \tag{4.3.3}$$

where $\overline{\gamma}_{r_{\mathbb{S}}d}$ is the mean channel power gain of $R_{\mathbb{S}} - D$ link.

Remarks: The outage-constrained EH relay transmissions in the second hop serve as an energy conservation strategy. Furthermore, the inclusion of it makes the end-to-end cooperative D2D communication policy novel and energy efficient. We note that the energy conservation strategy requires CSI of the second hop link. We note that the channel power gain threshold γ_0 depends on average channel power gain and p_0. Note that $\gamma_0 \to 0$ as $p_0 \to 0$. Thus, the energy efficient end-to-end green cooperative D2D communication policy considers the channel conditions local to the selected relay.

Remarks on the complexity analysis for OC-EHRS policy: For the OC-EHRS policy, three crucial tasks account for computing complexity. These tasks are CSI acquisition via estimation, relay selection, and outage-constrained signal transmission at the selected relay. The computational complexity of the CSI acquisition depends on the channel estimation algorithm. Since L relays are considered in the system model, optimal sorting algorithms can be employed to determine the relay that harvests maximum energy. Therefore, for the heap sorting algorithm, the computational complexity will be $\mathcal{O}(L \log_2(L))$ [111]. Furthermore, since the outage-constrained transmission is employed, the relay will check for the outage probability of the relay to the destination link. Since outage probability depends on the exponential term, its computational complexity will be $\mathcal{O}(\log_2^2(n))$ [130]. Therefore, the total complexity of the OC-EHRS policy will be the sum of the complexity accounted for from CSI acquisition, searching for the relay, which harvests maximum energy and outage constrained transmission.

In the following sections, we consider each of the objectives and present performance analysis of the above proposed green cooperative D2D communication policy.

4.4 Link Outage Analysis

Outage probability is a vital PHY layer performance measure of wireless systems. In the design of wireless systems, an outage probability of 0.01 is a typical target [100]. This section deals with the analysis of outage probability for $R_{\mathbb{S}}-D$ link, where $R_{\mathbb{S}}$ is the selected EHRN in the system model. Note that the EH relay selection reduces synchronization problem and hardware complexity [69]. Furthermore, selecting the relay that harvests maximum energy improves the performance of the system.

Let α is a unit energy information symbol. The selected EH relay forwards its received signal to the destination node. We note that EH relays are implementation-friendly and need not consume its harvested energy for additional processing tasks. Note that $h_{r_{\mathbb{S}}d}$ is the channel gain for the $R_{\mathbb{S}}-D$ link. Further, we assume statistically independent frequency-flat Rayleigh fading channel model for all the links. Therefore, the signal received at the destination node is given by

$$y_{r_{\mathbb{S}}d} = \sqrt{\mathcal{A}\ (\mathcal{EH}_{\max})} h_{r_{\mathbb{S}}d}\ \alpha + n_d, \tag{4.4.1}$$

where $n_d \sim \mathcal{CN}(0, \sigma_d^2)$ is the additive noise component.

For the $R_{\mathbb{S}}$−D link, the instantaneous SNR is given by

$$\Gamma_D = \frac{\mathcal{A} \max\{\mathcal{EH}_1, \mathcal{EH}_2, \ldots, \mathcal{EH}_L\}\ \gamma_{r_{\mathbb{S}}d}}{\sigma_d^2 \mathcal{D}^{\nu}}, \tag{4.4.2}$$

where $\mathcal{D}$ is the distance between the strongest EHRN and the destination node, $|h_{r_{\mathbb{S}}d}|^2 \triangleq \gamma_{r_{\mathbb{S}}d}$ be the instantaneous channel power gain of $R_{\mathbb{S}}$−D link, and $\overline{\gamma}_{r_{\mathbb{S}}d}$ is the corresponding mean channel power gain of the $R_{\mathbb{S}}$−D link.

Note that $\gamma_{r_{\mathbb{S}}d}$ is exponentially distributed and statistically independent with respect to maximum harvested energy. Furthermore, if Γ_{th} is the threshold SNR at the destination, then $\mathcal{P}(\Gamma_D < \Gamma_{\text{th}})$ denotes the outage probability for the $R_{\mathbb{S}}$−D link [100].

The link outage probability is given by

$$\begin{aligned}\mathcal{P}(\Gamma_D < \Gamma_{\text{th}}) = \mathcal{P}(\Gamma_D < \Gamma_{\text{th}} | \gamma_{r_{\mathbb{S}}d} \geq \gamma_0) \mathcal{P}(\gamma_{r_{\mathbb{S}}d} \geq \gamma_0) \\ + \mathcal{P}(\Gamma_D < \Gamma_{\text{th}} | \gamma_{r_{\mathbb{S}}d} < \gamma_0) \mathcal{P}(\gamma_{r_{\mathbb{S}}d} < \gamma_0).\end{aligned} \tag{4.4.3}$$

For $\gamma_{r_{\mathbb{S}}d} < \gamma_0$, $\Gamma_D = 0$ since $\mathcal{A} = 0$. Therefore, we have

$$\mathcal{P}(\Gamma_D < \Gamma_{\text{th}}) = e^{-\frac{\gamma_0}{\overline{\gamma}_{r_{\mathbb{S}}d}}}\ \mathcal{P}(\Gamma_D < \Gamma_{\text{th}} | \gamma_{r_{\mathbb{S}}d} \geq \gamma_0) \mathcal{P}(\gamma_{r_{\mathbb{S}}d} \geq \gamma_0), \tag{4.4.4}$$

where $\Gamma_D = \frac{\max\{\mathcal{EH}_1, \mathcal{EH}_2, \ldots, \mathcal{EH}_L\}\ \gamma_{r_{\mathbb{S}}d}}{\sigma_d^2 \mathcal{D}^{\nu}}$.

Below, we present an analytical result on the link outage probability.

Lemma 4.4.1 *Let* $k \triangleq \frac{\eta P_s}{d^{\nu}} \upsilon T$. *For the proposed outage-constrained transmission policy, the link outage probability is given by*

$$\mathcal{P}(\Gamma_D < \Gamma_{th}) = b\, e^{-\frac{\gamma_0}{\overline{\gamma}_{r_{\mathbb{S}}d}}} \int_0^{\infty} \left(1 - e^{-\frac{a}{y}}\right)^L e^{-by}\, dy \triangleq p_{out}^{r_{\mathbb{S}}-D}, \tag{4.4.5}$$

where $a = \frac{\Gamma_{th}}{k\mathcal{C}\overline{\gamma}}$, $b = \frac{1}{\overline{\gamma}_{r_{\mathbb{S}}d}}$, $\mathcal{C} = \frac{1}{\mathcal{D}^{\nu}\sigma_d^2}$ *and* $\overline{\gamma}$ *is the mean channel power gain of* $S - R_{\mathbb{S}}$ *link. Furthermore, for* $L = 1$ *and* $\gamma_0 = 0$, *the outage probability expression simplifies to*

$$p_{out}^{r_{\mathbb{S}}-D} = 1 - \sqrt{\frac{4\Gamma_{th}}{\mathcal{C}k\overline{\gamma}\ \overline{\gamma}_{r_{\mathbb{S}}d}}}\ \mathrm{K}_1\left(\sqrt{\frac{4\Gamma_{th}}{\mathcal{C}k\overline{\gamma}\ \overline{\gamma}_{r_{\mathbb{S}}d}}}\right), \tag{4.4.6}$$

where $\mathrm{K}_1(\cdot)$ *is the modified Bessel function of second kind and first order. Proof of the above expression is shown in appendix C.2.*

Remarks: We note that the link outage probability reduces due to the constrained transmissions based on channel conditions. The general analytical expression for the outage probability has a single integral, which we evaluate numerically. Note that the result is valid for Rayleigh fading with the simplified path loss model. In the presence of shadow fading, we observe further degradation in outage performance due to decreased end SNR. We note that, for $L = 1$, we have an upper bound. As the number of EHRNs L increases, link outage decreases.

We note that a 1% outage probability is a typical target in wireless systems [100]. Therefore, it is reasonable to choose the system design parameters such as threshold, the number of relays optimally to meet the target outage. By using multiple antennas at the source and destination, and with beamforming, it is possible to improve outage performance significantly. However, the improvement in outage performance comes with the expense of hardware complexity and accurate CSI requirement.

Remarks on EH subsystem parameter υ: As mentioned before, in this work, we do not focus on the optimization of the EH model parameter υ. However, observing the fact that the outage probability is a function of υ, one can obtain an estimate of υ by solving the outage equation numerically.

4.4.1 Asymptotic Link Outage Analysis

Consider the following scaling regime. Let the mean channel power gains and γ_0 are fixed. The source transmit power $P_s \to \infty$. Assume that the EH model parameters such as υ and T, all distances, path loss exponent, L, and Γ_{th} are all fixed. Furthermore, the relays have sufficiently large energy storage capacity.

Let $p_{\mathbb{A},\text{out}}^{r_{\mathbb{S}}-D}$ denote the asymptotic outage probability. In the asymptotic regime, we have

$$p_{\mathbb{A},\text{out}}^{r_{\mathbb{S}}-D} = \lim_{P_s \to \infty} b e^{-\frac{\gamma_0}{\overline{\gamma}_{r_{\mathbb{S}}d}}} \int_0^\infty \left(1 - \exp\left(-\frac{a}{y}\right)\right)^L e^{-by}\, dy, \tag{4.4.7}$$

As $P_s \to \infty$, we have $k \triangleq \frac{\eta P_s}{d^\nu} \upsilon T \to \infty$, which implies $a = \frac{\Gamma_{\text{th}}}{kC\overline{\gamma}} \to 0$. Therefore, $\left(1 - \exp\left(-\frac{a}{y}\right)\right) \approx \epsilon$, where ϵ is arbitrarily very small positive real constant. Furthermore, in the asymptotic regime, $\lim_{L\to\infty} \epsilon^L \to 0$. Therefore, we conclude that, for the green cooperative D2D wireless systems with a very large number of EHRNs, outage probability is zero in the proposed scaling regime in the asymptotic sense.

4.5 Average Spectral Efficiency Analysis

Considering the energy conserving transmission policy, we analyze two other significant PHY layer performance measures, namely, spectral efficiency and energy efficiency. In this section, we derive analytical expressions for the exact FASE, it's upper bound and asymptotic expression of FASE in high SNR regime.

For a given bandwidth, FASE gives knowledge regarding the capability of achieving the information rate in the green cooperative D2D wireless system. To determine FASE, we take the statistical average of instantaneous spectral efficiency with respect to channel fading. Mathematically, FASE can be expressed as

$$\overline{\mathcal{S}} = \mathbf{E}[\log_2(1 + \Gamma_D)] = (\log_2 e)\mathbf{E}[\ln(1 + \Gamma_D)]. \tag{4.5.1}$$

Note that FASE is a function of instantaneous SNR, which is given by (4.4.2). Below, we state an analytical result on the exact FASE.

Result 13 *Let $k \triangleq \frac{\eta P_s}{d^\nu}\upsilon T$. The exact FASE for the proposed policy is given by*

$$\begin{aligned}\overline{\mathcal{S}} = \frac{L e^{-\frac{\gamma_0}{\overline{\gamma}_{r_{\mathbb{S}}d}}}}{(\ln 2)\ \overline{\gamma}} \left[\int_{\gamma=0}^{\infty} e^{-\frac{\gamma}{\overline{\gamma}}} \left(1 - e^{-\frac{\gamma}{\overline{\gamma}}}\right)^{L-1} \ln(1 + \mathbb{C}_1\ \gamma\ \gamma_0)\, d\gamma \right] \\ + \frac{L}{(\ln 2)\ \overline{\gamma}} \left[\int_{\gamma=0}^{\infty} e^{\frac{1}{\mathbb{C}_1 \gamma\ \overline{\gamma}_{r_{\mathbb{S}}d}}} e^{-\frac{\gamma}{\overline{\gamma}}} \left(1 - e^{-\frac{\gamma}{\overline{\gamma}}}\right)^{L-1} \mathrm{E}_1\left(\frac{1 + \mathbb{C}_1\gamma\ \gamma_0}{\mathbb{C}_1\gamma\ \overline{\gamma}_{r_{\mathbb{S}}d}}\right) d\gamma \right],\end{aligned} \tag{4.5.2}$$

where $\mathbb{C}_1 = \frac{k}{\sigma_d^2 D^\nu}$, $\mathrm{E}_1(.)$ is the exponential integral, γ and $\overline{\gamma}$ is the instantaneous channel power gain and mean channel power gain of the $S - R_{\mathbb{S}}$ link respectively. The proof is relegated in appendix C.3.

Remarks on exact FASE: Note that the above analytical expression is valid for independent and identically distributed (i.i.d) channels. For non-identical, statistically independent channels, we get a more complicated analytical result for the exact FASE. We also note that further simplification of the single integral expression for FASE is not possible. Hence, we evaluate the exact FASE numerically. We find that the exact FASE depends on various EH model parameters, average channel power gains, number of relays L, and the outage constraint. Furthermore, we see that the exact FASE performance improves with the number of EH relays. To gain further insights, we derive an insightful closed-form upper bound for the exact FASE.

Remarks on impact of L on the system model: Note that the analytical results derived are a generalized expression for the L number of relays. In practice, deploying a large number of relays in the system will increase the performance of the system model. However, the large L increases the cost and computational time complexity at the source node, at which the relay selection takes place.

4.5.1 Upper Bound for Exact FASE

We use Jensen's inequality to derive the upper bound of FASE. Applying the inequality, exact FASE can be upper bounded as

$$\overline{\mathcal{S}} \leq \log_2(1 + \mathbf{E}[\Gamma_D]) \triangleq \overline{\mathcal{S}}_{\text{UB}}. \tag{4.5.3}$$

Below, we state the simplified closed-form expression for the upper bound FASE.

Result 14 *Let* $k \triangleq \frac{\eta P_s}{d^\nu} \upsilon T$ *and* $\mathbb{C}_1 = \frac{k}{\sigma_d^2 \mathcal{D}^\nu}$. *For the proposed policy, the exact FASE can be upper bounded as follows.*

$$\overline{\mathcal{S}} \leq \overline{\mathcal{S}}_{UB} = \log_2 \left(1 + \mathbb{C}_1 \mathbb{J} e^{-\frac{\gamma_0}{\overline{\gamma}_{r_{\mathbb{S}}d}}} \overline{\gamma}\ \overline{\gamma}_{r_{\mathbb{S}}d} \right), \tag{4.5.4}$$

where $\mathbb{J} = \sum_{m=1}^{L} \frac{1}{m}$. *The derivation is presented in appendix C.4.*

Remarks on the FASE upper bound: Note that the upper bound is in closed-form. Unlike the exact FASE expression, the upper bound has a much simpler form. However, $\overline{\mathcal{S}}_{\text{UB}}$ also depends on various EH system parameters and mean channel power gains. We evaluate the accuracy of the upper bound in section 4.7. Note that all the system parameters on which the upper bound depends are inside the logarithm. To get explicit dependence on the system model parameters, we present an asymptotic analysis in an interesting scaling regime.

4.5.2 Asymptotic FASE Analysis

For the proposed green cooperative D2D communication policy, we analyze asymptotic FASE in an interesting scaling regime. Let mean channel power gain of all the links are equal and fixed to $\overline{\gamma}$. Furthermore, the source transmit power P_s is assumed to be very large. We also assume, $p_0 \to 0$, therefore, we have $\gamma_0 = 0$. Let $\overline{\mathcal{S}}_{\mathbb{A}}$ be the asymptotic FASE. Below, we present an analytical result for $\overline{\mathcal{S}}_{\mathbb{A}}$.

Result 15 *Let* $k \triangleq \frac{\eta P_s}{d^\nu} \upsilon T$ *and* $\mathbb{C}_1 = \frac{k}{\sigma_d^2 \mathcal{D}^\nu}$. *In the scaling regime, the asymptotic FASE* ($\overline{\mathcal{S}}_{\mathbb{A}}$) *is given by*

$$\overline{\mathcal{S}} \leq \overline{\mathcal{S}}_{UB} \leq \overline{\mathcal{S}}_{\mathbb{A}} = \mathbb{C}_1 (\log_2 e) \overline{\gamma}\ \overline{\gamma}_{r_{\mathbb{S}}d} \left(\sum_{m=1}^{L} \frac{1}{m} \right). \tag{4.5.5}$$

The proof of this result is shown in appendix C.5.

Remarks on asymptotic FASE: The asymptotic expression usefulness lies in showing the explicit dependence of the system model parameters. For very large L, that is, as $L \to \infty$, $\sum_{m=1}^{L} \frac{1}{m} \approx \int_1^L \ln t \, dt = \ln L$. Therefore, we get $\overline{\mathcal{S}}_{\mathbb{A}} \approx (\log_2 e)\mathbb{C}_1 \overline{\gamma}\, \overline{\gamma}_{r\mathbb{S}d} \ln L$. In other words, given the fixed mean channel conditions and the fixed EH model parameters, the asymptotic spectral efficiency $\propto \log_2 L$.

4.6 Average Energy Efficiency Analysis

In this section, we derive analytical results on the exact FAEE, its upper bound, and asymptotic energy efficiency. FAEE serves as another critical PHY layer performance measure. It provides insights regarding the efficient utilization of the energy by the proposed wireless system. Energy efficiency ($\mathcal{E}$) is a closely related performance parameter of spectral efficiency. It is the ratio of spectral efficiency to the total power consumed in the network. FAEE can be mathematically represented as

$$\overline{\mathcal{E}} = \frac{\mathbf{E}\,(\mathcal{S})}{\mathbf{E}\,(P_{\mathrm{T}})} = \frac{\mathbf{E}[\log_2(1+\Gamma_D)]}{\mathbf{E}\,(P_{\mathrm{T}})}, \tag{4.6.1}$$

where P_{T} is the total power consumed in the green cooperative D2D system.

Power consumption model: The total power is the sum of three power components. Mathematically, P_{T} is given by

$$P_{\mathrm{T}} = P_s + P_r + P_c, \tag{4.6.2}$$

where P_s is the source transmit power, P_r is the relay transmit power and P_c is the power consumed by the circuitry. Further, relay transmit power can be expressed as

$$P_r = \frac{\mathcal{A}\ \max\{\mathcal{EH}_1, \mathcal{EH}_2, \ldots, \mathcal{EH}_L\}}{\frac{(1-\upsilon)T}{2}}. \tag{4.6.3}$$

Below, we state an insightful analytical result on the exact FAEE. To gain more insights, we also derive closed-form upper bound for FAEE and asymptotic FAEE expressions.

Result 16 *Let $k \triangleq \frac{\eta P_s}{d^\nu}\upsilon T$ and $\mathbb{C}_1 = \frac{k}{\sigma_d^2 D^\nu}$. The exact FAEE for the proposed policy is given by*

$$\overline{\mathcal{E}} = \left[\frac{L e^{-\frac{\gamma_0}{\overline{\gamma}_{r\mathbb{S}d}}}}{\ln(2)\,\overline{\gamma}} \int_{\gamma=0}^{\infty} e^{-\frac{\gamma}{\overline{\gamma}}} \left(1 - e^{-\frac{\gamma}{\overline{\gamma}}}\right)^{L-1} \ln(1 + \mathbb{C}_1\gamma\ \gamma_0)\, d\gamma + \frac{L}{\ln(2)\,\overline{\gamma}} \int_{\gamma=0}^{\infty} e^{\frac{1}{\mathbb{C}_1\gamma\ \overline{\gamma}_{r\mathbb{S}d}}} e^{-\frac{\gamma}{\overline{\gamma}}} \times \left(1 - e^{-\frac{\gamma}{\overline{\gamma}}}\right)^{L-1} \times \mathrm{E}_1\left(\frac{1 + \mathbb{C}_1\gamma\ \gamma_0}{\mathbb{C}_1\gamma\ \overline{\gamma}_{r\mathbb{S}d}}\right) d\gamma\right] \times \left[\frac{\frac{(1-\upsilon)T}{2}}{(P_s + P_c)\frac{(1-\upsilon)T}{2} + k\overline{\gamma}\mathbb{J}\exp\left(-\frac{\gamma_0}{\overline{\gamma}_{r\mathbb{S}d}}\right)}\right], \tag{4.6.4}$$

where $\mathbb{J} = \sum_{m=1}^{L} \frac{1}{m}$. *Proof is relegated in appendix C.6.*

Remarks on exact FAEE: Note that the above analytical expression is valid for i.i.d channels. For non-identical, statistically independent fading channels, we get a more complicated analytical result for the exact FAEE. We note that further simplification of FAEE expression is not possible. Therefore, we evaluate the exact FAEE numerically. Similar to the exact FASE, the exact FAEE also depends on various system parameters. However, FAEE also depends on the power consumption model parameters. We evaluate the performance of FAEE in section 4.7. To gain further insights, we derive an insightful closed-form upper bound for the exact FAEE.

4.6.1 Closed-form Upper Bound for FAEE

To derive closed-form upper bound for the FAEE, we apply Jensen's inequality on the numerator term of equation (4.6.1). Below, we state the result on closed-form upper bound.

Result 17 *Let* $k \triangleq \frac{\eta P_s}{d^{\nu}} \upsilon T$ *and* $\mathbb{C}_1 = \frac{k}{\sigma_d^2 D^{\nu}}$. *For the proposed policy, the exact FAEE can be upper bounded as follows.*

$$\overline{\mathcal{E}}_{UB} = \frac{\frac{(1-\upsilon)T}{2} \; \log_2\Big(1 + \mathbb{C}_1 \mathbb{J} \exp\Big(-\frac{\gamma_0}{\overline{\gamma}_{r_{\mathbb{S}}d}}\Big)\overline{\gamma}\;\overline{\gamma}_{r_{\mathbb{S}}d}\Big)}{(P_s + P_c)\frac{(1-\upsilon)T}{2} + k\overline{\gamma}\mathbb{J}\exp\Big(-\frac{\gamma_0}{\overline{\gamma}_{r_{\mathbb{S}}d}}\Big)}, \tag{4.6.5}$$

where $\mathbb{J} = \sum_{m=1}^{L} \frac{1}{m}$. *The Proof is relegated in appendix C.7.*

Remarks on the FAEE upper bound: Note that the FAEE upper bound is in closed-form. Unlike the exact FAEE expression, the upper bound is simpler and easier to evaluate. We evaluate the accuracy of the FAEE upper bound in section 4.7. To get more explicit dependence on the system model parameters, we present an asymptotic analysis in an interesting scaling regime.

4.6.2 Asymptotic FAEE Analysis

For the proposed green cooperative D2D communication policy, we analyze asymptotic FAEE in the scaling regime mentioned before. Let $\overline{\mathcal{E}}_{\mathbb{A}}$ be the asymptotic FAEE. Below, we present an analytical result for $\overline{\mathcal{E}}_{\mathbb{A}}$.

Result 18 *Let* $k \triangleq \frac{\eta P_s}{d^{\nu}} \upsilon T$ *and* $\mathbb{C}_1 = \frac{k}{\sigma_d^2 D^{\nu}}$. *In the scaling regime, the asymptotic*

FAEE is given by

$$\overline{\mathcal{E}}_{\mathbb{A}} = \frac{(\log_2 e)\, \mathbb{C}_1 \overline{\gamma}\ \overline{\gamma}_{r\mathbb{S}d} \left(\sum_{m=1}^{L} \frac{1}{m}\right) \frac{(1-v)T}{2}}{(P_s + P_c)\frac{(1-v)T}{2} + k\overline{\gamma}\left(\sum_{m=1}^{L} \frac{1}{m}\right)}. \tag{4.6.6}$$

The proof is shown in appendix C.8.

Remarks on asymptotic FAEE: The asymptotic expression usefulness lies in showing the explicit dependence of all the system model parameters, including the power consumption model. For large L, that is, as $L \to \infty$, we have $\sum_{m=1}^{L} \frac{1}{m} \approx \ln L$. Therefore, we have

$$\overline{\mathcal{E}}_{\mathbb{A}} \approx \frac{(\log_2 L)\, \mathbb{C}_1 \overline{\gamma}\overline{\gamma}_{r\mathbb{S}d} \frac{(1-v)T}{2}}{(P_s + P_c)\frac{(1-v)T}{2} + k\overline{\gamma}\ln L}. \tag{4.6.7}$$

4.7 Numerical Results and Interpretation

In this section, we first numerically evaluate and plot the statistical average $\overline{\mathcal{EH}}_{\max}$. Furthermore, we obtain several numerical results to validate the derived analytical expressions for the outage probability, FASE, and FAEE. To verify the mathematical expressions, we perform Monte-Carlo simulations. Before presenting the plots, we briefly explain the simulation methodology.

4.7.1 Simulation Methodology and Parameters

Initial parameter declaration: Table 4.1 presents the list of simulation parameters considered for generating plots. We have used representative parameters (for example, $d = \mathcal{D} = 1$ m or $\eta = 80\%$) to quantify the performance gains achieved by the proposed policies. Note that the trend of the plots will remain unchanged by scaling up the distance as it causes more path loss. Moreover, such assumptions for d or $\mathcal{D}$ are valid for indoor scenarios, for example, the literature where practical test-beds are set up to analyze the performance of cooperative communication for indoor environments [131–134]. Furthermore, as far as the energy conversion efficiency is concerned, it is possible to have η close to 80% with more sensitive energy harvesting circuitry [135].

Note that we mention simulation specific parameters inside the captions of the simulation results. A summary of the simulation methodology is as follows.

Data symbol generation at the source: We generate 10^5 equally likely real data symbols, which are having unit energy. We assume that the source transmits with fixed power P_s.

Table 4.1: Simulation parameters for green cooperative D2D communication system.

Symbol	Simulation Parameter	Value
N	Number of channel realizations	10^5
L	Number of relays	2
T	Time Slot	1 s
υ	Energy harvesting duty cycle	0.4
η	Energy conversion efficiency	80%
p_0	Outage constraint	0.01
P_c	Power consumed by the circuitry	15 dBm
d	Source node to relay node distance	1 m
$\mathcal{D}$	Relay node to destination node distance	1 m
ν	Path loss exponent	2.7
$\lvert\alpha\rvert^2$	Symbol energy	1

Fading channel and noise realizations : We generate 10^5 fading channel and noise realizations according to frequency-flat Rayleigh fading and AWGN.

Relay EH profile, relay selection policy with energy conservation strategy: Each relay node harvests a certain amount of energy, which is given by $\mathcal{EH}_n = \frac{\eta P_s \gamma_n}{d_n^{\nu}} \upsilon T$. For each fading channel realization, we select a non-regenerative EH relay that harvests maximum instantaneous energy. The selected relay participate in the relaying process with a constraint that the channel power gain of $R_{\mathbb{S}} - D$ link should be greater than the threshold γ_0 of $R_{\mathbb{S}} - D$ link.

Evaluation of performance measures at the destination: For each channel realization, we determine the presence or absence of the outage event. For the number of channel realizations, we then compute the average outage probability. Similarly, for each channel realization, we first calculate instantaneous spectral efficiency and energy efficiency. Finally, for the number of channel realizations, we evaluate FASE and FAEE and compare them with that of the benchmark RRS policy.

4.7.2 Impact of Mean Channel Gain on $\overline{\mathcal{EH}}_{\max}$

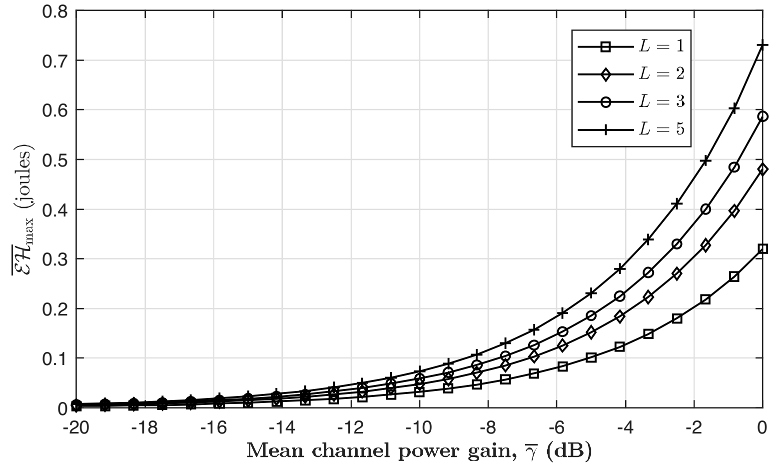

Figure 4.3: Rayleigh fading plus path loss model (absence of shadowing): $\overline{\mathcal{EH}}_{\max}$ as a function of mean channel power gain ($\upsilon = 0.4$, $d = 1$ m, $\eta = 0.8$, and $P_s = 0$ dB.).

Figure 4.3 plots $\overline{\mathcal{EH}}_{\max}$ as a function of mean channel power gain for different L. Note that only Rayleigh fading with path loss (absence of shadowing) is considered in the figure. Therefore, the mathematical expression for the average maximum harvested energy becomes $\overline{\mathcal{EH}}_{\max} = (\frac{\eta P_s \overline{\gamma}}{d^{\nu}})\upsilon T \sum_{m=1}^{L}(\frac{1}{m})$. It can be deduced from the mathematical expression, that if the value of L increases, the $\overline{\mathcal{EH}}_{\max}$ also increase, which can also be observed from the figure. However, this leads to increased system complexity. Further, with the increase in the mean channel power gain of the source to the relay link, the mean harvested energy by the relay nodes also increase because of good channel conditions. Hence $\overline{\mathcal{EH}}_{\max}$ increases monotonically with respect to the mean channel power gain. Note that the presence of shadow fading also shows a similar trend. However, $\overline{\mathcal{EH}}_{\max}$ is affected when the RF signal path undergoes shadowing.

4.7.3 Evaluation of Link Outage Probability

Our primary focus is on average energy efficiency and explicitly show the performance gains achieved by our proposed policy in terms of energy efficiency. However, we also present numerical results on outage probability and spectral efficiency to get more insights. Specifically, to understand the performance trade-off between average energy efficiency and average spectral efficiency.

We consider two benchmark policies for comparing numerical results on outage probability, spectral efficiency, and energy efficiency. The two benchmark policies are the partial relay selection policy [136] and RRS policy [76, 136]. In the partial relay selection policy, the EH relay is selected based on the instantaneous SNRs of links between the source node and the relay nodes. Hence the relay having maximum instantaneous SNR of source node to itself is selected to forward the signal. Unlike this benchmark policy, our proposed outage constrained, energy efficient cooperative D2D communication policy consists of two parts: i). EH relay selection based on energy harvested in a particular slot and ii). Outage based relaying to conserve energy in poor channel conditions.

On the other hand, in the random EH relay selection policy, the EH relay is selected randomly (independent of channel statistics and energy harvested) to process and forward its received signal to the destination. Our proposed policy differs from the random EH relay selection policy in several ways. Firstly, our policy considers harvested energies that depend on channel conditions, and secondly, the outage constrains the selected EH relay transmissions. Thus, the novelty in our work fundamentally lies in outage-constrained relaying. Below, we present an outage performance plot with benchmarking.

Outage performance benchmarking and comparisons:

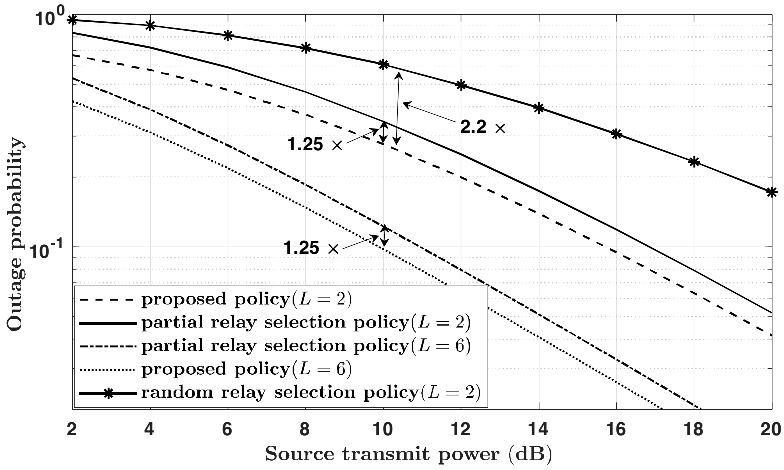

Figure 4.4: Outage probability as a function of source transmit power ($\upsilon = 0.4$, $p_0 = 0.2$, $d = 1$ m, $\eta = 0.8$, average channel power gain of all links = 1, $\mathcal{D} = 1$ m, and $\sigma_d = 1$.).

Figure 4.4 plots outage probability with respect to source transmit power for different L. The figure compares the outage performance of the proposed outage-constrained, green cooperative D2D communication policy and the benchmark policies. The initial observation is that, as the source transmit power increases, all the policies outage probability decreases. This trend is due to the modified Bessel function of the second kind in (4.4.6) at high source transmit power. Further, we find that as L increases, the outage probability decreases, as expected. This improvement in outage performance is due to the improved average amount of maximum energy harvested for large L. However, the improved outage performance comes with the higher hardware complexity and processing burden of the green cooperative D2D radio system with many EH relays. Further, since the transmission of the proposed policy is outage constrained, its performance is better than both the benchmark policies. Quantitatively we observe that the proposed policy perform approximately 1.25 times better in comparison to partial relay selection policy at $P_s = 10$ dB. Lastly, proposed policy perform approximately 2.2 times better in comparison to random relay selection policy at $P_s = 10$ dB.

Remarks: Note that the random EH relay selection policy is insensitive to L because of the following reasons. Since we have assumed i.i.d channel gains for all links, the RRS is insensitive to L. Furthermore, the EH relay selection is independent of the amount of energy harvested in a time slot. However, one can expect the dependency of L on outage probability in non-i.i.d scenarios due to the chances of selecting the EH relay with higher mean channel power gain.

4.7.4 Numerical Results on FASE with Benchmarking

Performance benchmarking and comparisons:

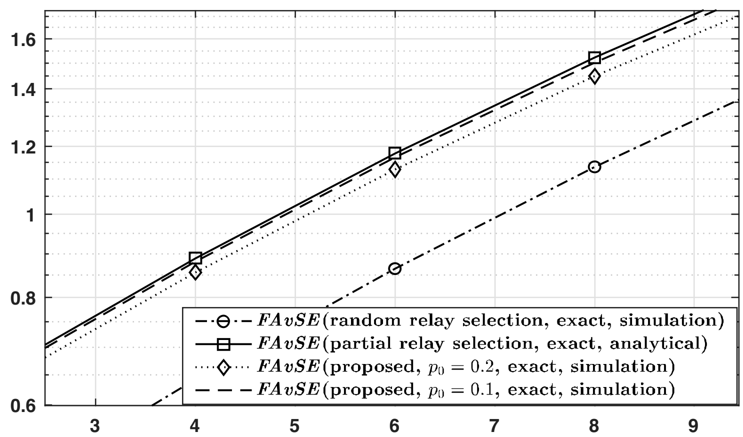

Figure 4.5: FASE as a function of source transmit power ($\upsilon = 0.4$, $d = 1$ m, $\eta = 0.8$, average channel power gain of all links = 1, $\mathcal{D} = 1$ m, $L = 2$, and $\sigma_d = 1$.).

Figure 4.5 plots FASE with respect to source transmit power for the proposed policy and the benchmark policies. The proposed green cooperative D2D radio communication policy is compared with two benchmark policies: partial relay selection policy and RRS policy. Since the proposed green cooperative D2D radio communication policy is outage constrained, therefore the performance of proposed policy is analyzed for two different outage probability values, that is, $p_0 = 0.1$ and $p_0 = 0.2$. We observe that the proposed green cooperative D2D radio communication policy's performance is better than the RRS policy for both the p_0 values. Furthermore, due to the outage constrained relay transmission of the proposed policy, its spectral efficiency performance shows little degradation compared to the partial relay selection policy. However, in the following figure, we show that the proposed green cooperative D2D communication policy is more energy efficient than the benchmark policies.

Remarks: Note that the proposed policy is not spectral efficient (though it is energy efficient, shown in the Figure 4.9) in comparison to the partial relay selection policy. However, during the outage, the partial relay selection policy is not reliable and energy efficient. Furthermore, the throughput, which is a function of link probability error (depends on modulation and coding schemes), will be low in poor channel conditions. Thus, the benchmark policies would consume the precious harvested energy by transmitting signals via the non-reliable, erroneous link between the selected EH relay and the destination.

Extensions and applications: To look in a different model and perspective, consider a cooperative D2D EH relays-assisted network with multiple destinations. In such a scenario, we can extend our proposed policy to choose the best (least outage) destination node to transmit the selected EH relay signal. Thus, the proposed green cooperative D2D radio communication policy is readily applicable to more complex green cooperative D2D networks.

Furthermore, consider the proposed green cooperative D2D model with multiple hybrid EH relays, where the relay can partially use the inbuilt battery in place of harvested energy during outage events. This replacement of pure EH relays by hybrid EH relays can enhance performance in terms of FASE and communication reliability. However, these improvements come at the expense of improved relaying complexity and cost.

Impact of P_s on FASE:

Figure 4.6 plots FASE as a function of source transmit power. It also plots FASE upper bound and the RRS policy. We observe that as the source transmit power increases, the FASE also increases. This trend happens because of the increase in the SNR at the destination led by the increase in source transmit power (can be analyzed from equation (4.5.4)). Further, we see that the exact FASE and the Monte-Carlo simulations match well. In the figure, we also observe that the upper bound tracks the exact FASE well. Furthermore, we see that the proposed policy significantly

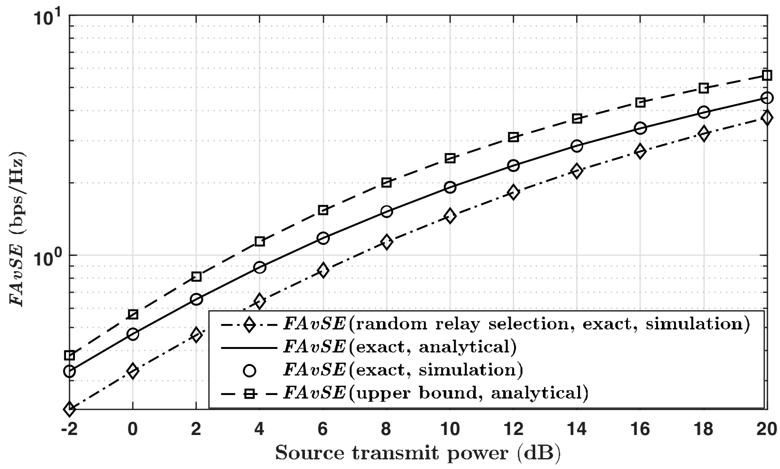

Figure 4.6: FASE as a function of source transmit power ($\upsilon = 0.4$, $d = 1$ m, $\eta = 0.8$, average channel power gain of all links $= 1$, $\mathcal{D} = 1$ m, $L = 2$, and $\sigma_d = 1.$).

outperforms the benchmark RRS policy.

Remarks on accuracy: The percentage deviation between values obtained from analytical results and simulations depends primarily on the following factors as described below.

i). Approximations: The approximations in analysis lead to more variation between analysis and simulation plots. Since we have not considered any approximations and modeled the proposed system exactly in our simulation, our analytical graphs closely match the simulation graphs.

ii). Channel realizations: According to the law of large numbers [137], the accuracy of the performance measure that we numerically evaluate via simulations improves with a large number of channel realizations or samples. Note that we have considered many channel realizations (that is 10^5). Therefore, the variation between analysis and simulation plot is significantly less or negligible.

Impact of mean $R_{\mathbb{S}} - D$ channel power gain on FASE:

Figure 4.7 plots FASE as a function of the average channel power gain of the $R_{\mathbb{S}} - D$ link. This figure shows the impact of mean channel power gain on FASE, and the upper bound. It also plots the average spectral efficiency of the random relay selection policy. As the average channel power gain increases, the FASE (can be analyzed from equation (4.5.4)) also increases because of the improvement in SNR at the destination. However, the rate of increase in FASE is relatively slow due to the performance measure's logarithmic nature.

Further, we see that the exact FASE and Monte-Carlo simulations match well. In the figure, we also observe the upper bound tracking the exact FASE well. Lastly, we see that the proposed policy outperforms the benchmark relay selection policy by a

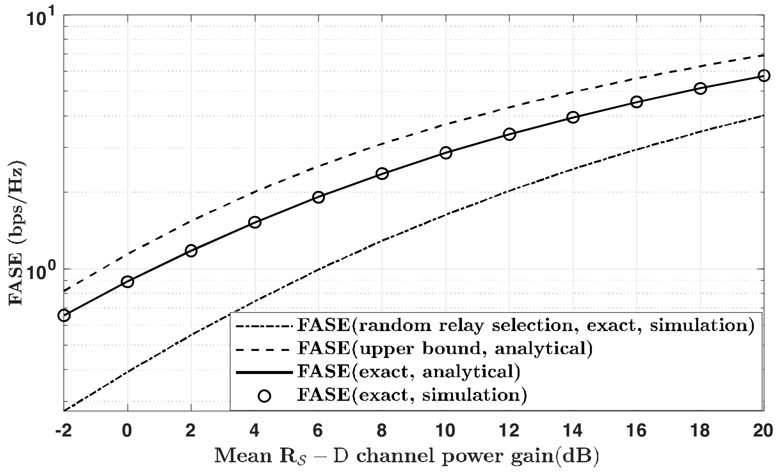

Figure 4.7: FASE as a function of average channel power gain of $R_{\mathbb{S}}-D$ link ($\upsilon = 0.4$, $d = 1$ m, $\eta = 0.8$, $P_s = 4$ dB, $\mathcal{D} = 1$ m, $L = 2$, and $\sigma_d = 1.$).

large margin for all mean channel power gains.

Impact of P_s and L on FASE:

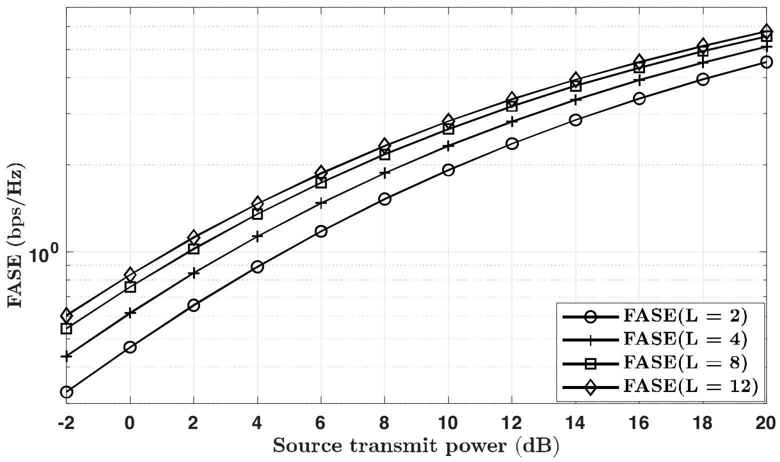

Figure 4.8: FASE as a function of source transmit power for various values of L ($\upsilon = 0.4$, $d = 1$ m, $\eta = 0.8$, average channel power gain of all links = 1, $\mathcal{D} = 1$ m, and $\sigma_d = 1.$).

Figure 4.8 plots FASE as a function of the source transmit power P_s for different L. This figure shows the impact of P_s and L on the exact FASE for the proposed policy. As P_s increases, the FASE also increases, as expected. Furthermore, from the analysis in section 4.1, we observe that as the source transmit power increases, the $\overline{\mathcal{EH}}_{\max}$ increases. This improvement in the $\overline{\mathcal{EH}}_{\max}$ causes the improvement in the SNR at the destination. Thus, we observe the enhanced FASE performance in the figure. We also observe that FASE increases rather slowly for large L. This gradual improvement in FASE as a function of L is due to its dependence logarithmically. Therefore, we need to choose L wisely to trade-off green cooperative D2D system complexity and performance.

4.7.5 Numerical Results on FAEE with Benchmarking

Performance benchmarking, comparisons, and gains:

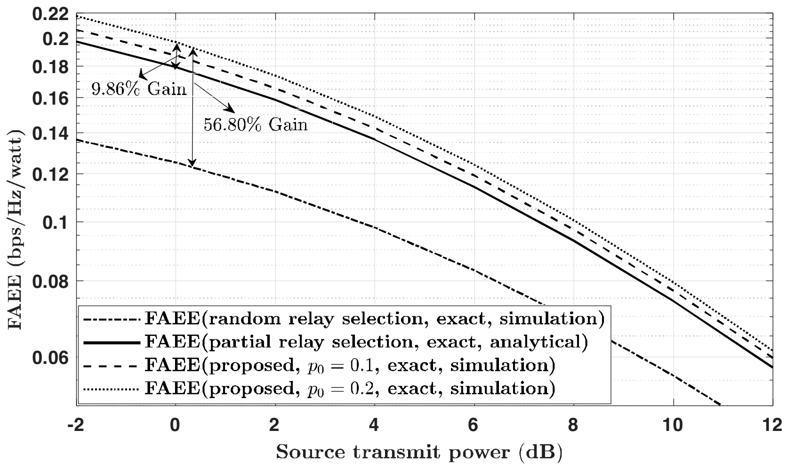

Figure 4.9: FAEE as a function of source transmit power ($\upsilon = 0.4$, $d = 1$ m, $\eta = 0.8$, average channel power gain of all links = 1, P_c = 15 dBm, $\mathcal{D}$ = 1 m, $L = 2$, and $\sigma_d = 1$.).

Figure 4.9 plots FAEE with respect to source transmit power for the proposed policy and the benchmark policies. The proposed outage-constrained, green cooperative D2D radio communication policy is compared with two benchmark policies: partial relay selection policy and RRS policy. Note that the proposed policy is analyzed for two different outage probability values, that are, $p_0 = 0.1$ and $p_0 = 0.2$. Further, we observe that the proposed policy for both the values of p_0 is performing better than the benchmark policies. The specific reason for the performance gain is power conservation based on the outage constraint. A performance gain of 9.86% in energy efficiency is achieved by the proposed policy with $p_0 = 0.2$ in comparison to the partial relay selection policy at $P_s = 0$ dB. Furthermore, the performance gain of 56.80% is achieved compared to the RRS policy.

Remarks: Note that, due to the outage-constrained relay transmissions, a substantial performance gain in terms of energy efficiency can be observed by the proposed green cooperative D2D communication policy when compared to the benchmark policies. Furthermore, for large scale cooperative multi-hop EH Internet of Things (IoT), the aggregate energy efficiency gains could be much higher for the proposed policy when compared to the benchmark policies. *Impact of P_s on FAEE:*

Figure 4.10 shows the impact of increasing the source transmit power P_s on FAEE. The figure also plots the upper bound and the benchmark policy. We see that as P_s

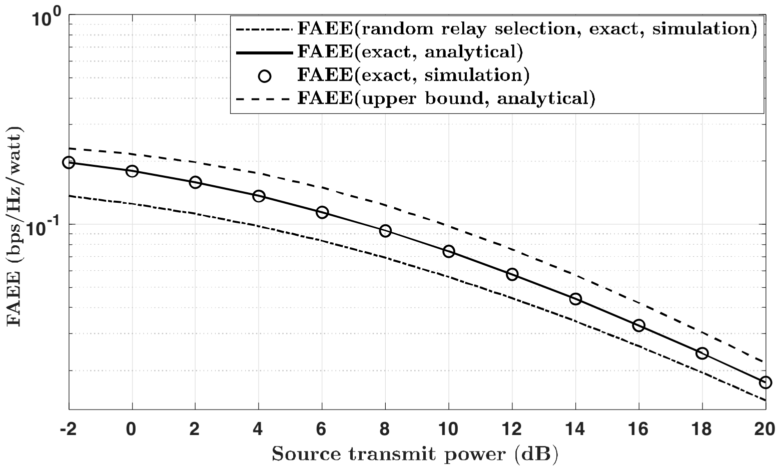

Figure 4.10: FAEE as a function of source transmit power ($\upsilon = 0.4$, $d = 1$ m, $\eta = 0.8$, average channel power gain of all links = 1, $P_c = 15$ dBm, $\mathcal{D} = 1$ m, $L = 2$, and $\sigma_d = 1.$).

increases, the FAEE of the proposed model decreases. This degradation in average energy efficiency is due to increased average total power consumption. The upper bound tracks the exact FAEE well. Furthermore, we see that the proposed policy outperforms the RRS policy.

Impact of mean $R_{\mathbb{S}} - D$ channel power gain on FAEE:

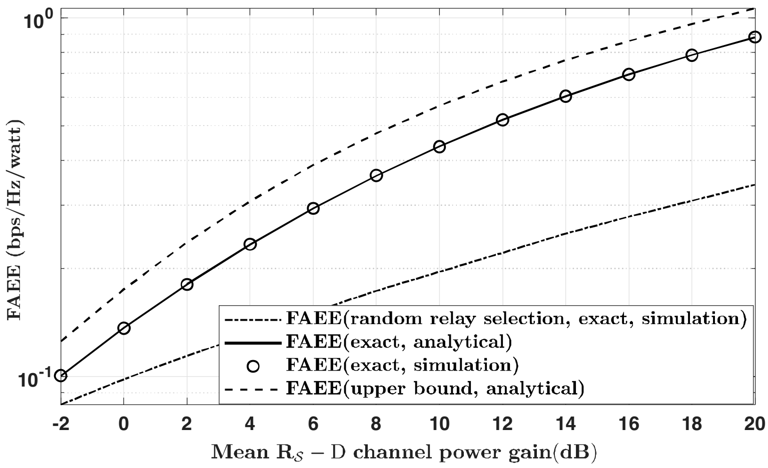

Figure 4.11: FAEE as a function of average channel power gain of $R_{\mathbb{S}} - D$ link ($\upsilon = 0.4$, $d = 1$ m, $\eta = 0.8$, $P_s = 4$ dB, $P_c = 15$ dBm, $\mathcal{D} = 1$ m, $L = 2$, and $\sigma_d = 1.$).

Figure 4.11 shows the impact of increasing average channel power gain of $R_{\mathbb{S}} - D$ link on FAEE. The figure also shows the upper bound and the benchmark policy. We see that as average channel power gain increases, the SNR of the signal received at the destination node increases, therefore the FAEE increases. However, the total average power consumption remains fixed. Note that the exact FAEE and Monte-Carlo simulation plot match well. In the Figure, the upper bound tracks the exact average energy efficiency curve well. Furthermore, the proposed energy efficiency green cooperative D2D policy outperforms the benchmark policy significantly.

Impact of P_s and L on FAEE:

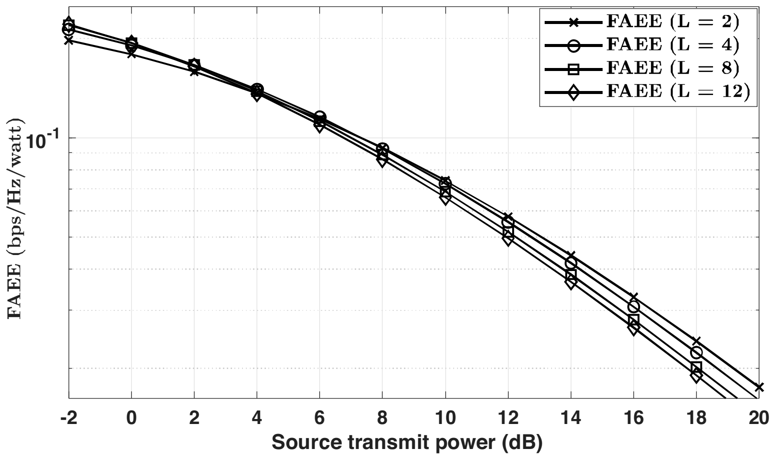

Figure 4.12: FAEE as a function of source transmit power for various values of L ($\upsilon = 0.4$, $d = 1$ m, $\eta = 0.8$, average channel power gain of all links = 1, $P_c = 15$ dBm, $\mathcal{D} = 1$ m, and $\sigma_d = 1$.).

Figure 4.12 shows the exact FAEE for increasing P_s for different L. The FAEE performance is better for high L at low P_s values. This trend continues till a few dBs of P_s because of different logarithmic dependence in the numerator and the denominator term, which can be seen in equation (4.6.7). On the other hand, at higher values of P_s, FAEE performance is poor due to increased total average power consumption.

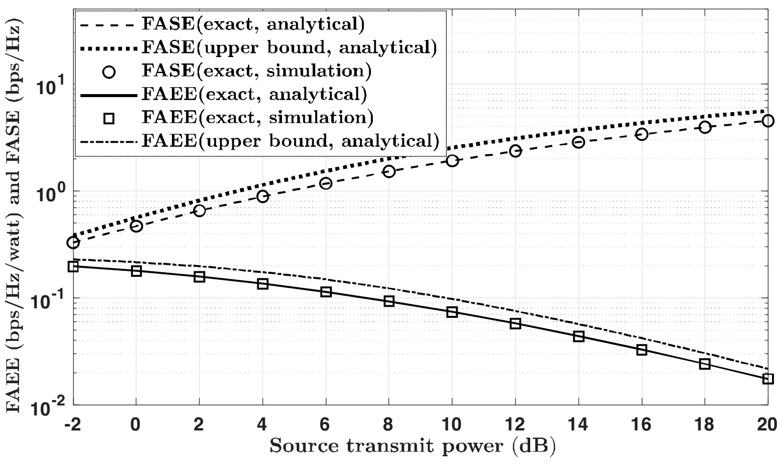

Figure 4.13: FASE and FAEE as a function of source transmit power ($\upsilon = 0.4$, $d = 1$ m, $\eta = 0.8$, average channel power gain of all links = 1, $P_c = 15$ dBm, $\mathcal{D} = 1$ m, $L = 2$, and $\sigma_d = 1$.).

FAEE − FASE *tradeoff*: Figure 4.13 plots both the average spectral efficiency and the average energy efficiency as functions of the source transmit power. This plot explicitly shows the tradeoff between FASE and FAEE. We see that, as P_s increases, FASE increases, as expected. On the other hand, as P_s increases, the total average power consumption in the system increases. Therefore, FAEE decreases.

Remarks: Note that a monotonically decreasing trend (for FAEE versus FASE) is similar to the behavior shown in the literature plot [138]. Thus, we validate the spectral efficiency and energy efficiency trade-off. The designer can appropriately adjust the regime to achieve the required spectral efficiency or energy efficiency depending on the system or network requirements.

4.8 Summary

In this chapter, we considered a green cooperative D2D wireless system that uses multiple time-switching based non-regenerative EH relays. In it, the relay nodes harvest energy from its received RF signal. Considering small scale fading and large scale fading with path loss, we developed a first-order statistical analysis of the maximum harvested energy. To gain more insights, we also evaluated the system performance in terms of outage probability, FASE, and FAEE. Specifically, we derived novel and insightful analytical expressions for exact performance measures and upper bounds. We also presented an insightful asymptotic analysis for these PHY layer performance measures. Based on the numerical results, we found that the relay selection policy outperforms the benchmark policies with respect to FAEE. We observe that the proposed policy achieves a performance gain of 9.86% in energy efficiency compared to the partial relay selection policy. Furthermore, the performance gain of 56.80% is achieved compared to the RRS policy. The substantial gains achieved by the green cooperative D2D system with relay selection motivate its use in green cooperative and cognitive radio systems. An interesting problem for future work is to determine the optimized value of υ for the TSP based on channel characteristics.